Invariant Averaging Over the Kottler Family of Solutions of the Einstein Vacuum Equation with a ±Λ-term

Mikhail Batanov-Gaukhman[1]

(1) Moscow Aviation Institute (National Research University),
Institute No. 2 "Aircraft and Rocket Engines and Power Plants",
4 Volokolamskoe Shosse, Moscow, Russia, 125993
(e-mail: alsignat@yandex.ru)

September 20, 2026

ABSTRACT

This article proposes treating the Kottler family of 10 metric solutions of the Einstein vacuum equation with a $\pm\Lambda$-term within a single system. To this end, we propose the invariant averaging of the scalars associated with each solution of this Kottler family. As a result, averaged scalars and curvature invariants of the region of space under study are obtained: $\langle C_{\mu\nu\rho\sigma}C^{\mu\nu\rho\sigma}\rangle = 12r_b^2/r^6$, $\langle R_{\mu\nu}R^{\mu\nu}\rangle = 36/r_a^4$, $\langle g_{00}\rangle = 1$, $\langle R\rangle = 0$, $\langle R_{00}\rangle = 3c^2r^2/r_a^4$, $\langle K\rangle = 12r_b^2/r^6 + 24/r_a^4$, $\langle l_r^{(+)}\rangle = \langle\frac{\Delta r}{r}\rangle = \langle\sqrt{g_{11}} - 1\rangle$ and others. On the basis of these averaging results, mathematical models of two mutually opposite stable spherical vacuum formations are considered, and contradictions of this method are identified. To overcome the resulting difficulties, an extended Einstein vacuum equation with a finite difference of a large number of positive and negative $\pm\Lambda$-terms is proposed. This approach may serve as a basis for a Hierarchical Cosmological Model, as part of a unified study entitled "Geometrized Vacuum Physics Based on the Algebra of Signatures", aimed at the development of the Clifford–Einstein–Wheeler program for the complete geometrization of physics.

Keywords: averaging problem, Kottler metric, Einstein manifold, de Sitter / anti-de Sitter space, metric signature, vacuum, metric solutions, vacuum equation, cosmological model, relative elongation of the vacuum

1 Introduction

The Einstein vacuum equation with a Λ-term (or Einstein manifold equation) has the form:

$$R_{ik} = \Lambda g_{ik}, \tag{1}$$

where g_{ik} are the components of the metric tensor of a smooth 4-dimensional space with the pseudo-Riemannian metric $ds^2 = g_{ik}\,dx^i dx^k$;

$R_{ik} = \frac{\partial \Gamma_{ik}^l}{\partial x^l} - \frac{\partial \Gamma_{il}^l}{\partial x^k} + \Gamma_{ik}^l\Gamma_{lm}^m - \Gamma_{il}^m\Gamma_{mk}^l$ – the Ricci tensor, (2)

$\Gamma_{ik}^\lambda = \frac{1}{2}g^{\lambda\mu}\left(\frac{\partial g_{\mu k}}{\partial x^i} + \frac{\partial g_{i\mu}}{\partial x^k} - \frac{\partial g_{ik}}{\partial x^\mu}\right)$ – the Christoffel symbols, (3)

$T_{ik} = 0$ – the zero energy–momentum tensor of an external material source (no source is present), (4)

$\Lambda = 3/r_a^2$ – a constant (where r_a is the radius of the sphere, or the de Sitter radius). (5)

The vacuum equation (1), as the result of solving the Einstein–Hilbert variational problem, rests on the following fundamental principles and axioms underlying modern physics [1–14]*: general covariance, coordinate invariance, equivalence, independence of the speed of light from the reference frame, causality, extremal action, relativity, quasi-linearity, diffeomorphism invariance, scale invariance, and self-consistency.

In addition, in the 3+1 ADM decomposition, the vacuum equation (1) is represented as a set of 4 constraint equations and 6 evolution equations, which resemble conservation laws, since

$$\nabla_j[R_{ik} - \Lambda g_{ik}] = 0. \tag{6}$$

The reason is that the tensor under consideration is identically zero ($R_{ik} - \Lambda g_{ik} = 0$): $\nabla_j 0 = \frac{\partial 0}{\partial x^j} - \Gamma_{ij}^l 0 - \Gamma_{kj}^l 0 = 0.$

However, in curved spacetime, obtaining integrals of motion from a divergence requires integration over a volume, but the covariant derivative contains Christoffel symbols, which prevent the application of the Gauss–Ostrogradsky theorem to tensors of rank two and higher (in particular, $\Gamma_{ik}^l\Gamma_{lm}^m - \Gamma_{il}^m\Gamma_{mk}^l$). Nevertheless, the vacuum equation (1) is suitable for identifying stable vacuum formations.

This combination of fundamental principles in a single vacuum equation (1) gives its solutions special significance.

2 Solutions of the Einstein Vacuum Equation with a Λ-Term

The generalized Birkhoff theorem* states that the only spherically symmetric solutions of equation (1)

$$R_{ik} - \Lambda g_{ik} = 0 \tag{7}$$

are given by the Kottler family of metrics* [1,2,5,13]

$$ds_1^2 = \pm f(r)c^2dt^2 \mp \frac{dr^2}{f(r)} \mp r^2 d\theta^2 \mp r^2 \sin^2\theta\, d\phi^2. \tag{8}$$

Of these, five metric solutions have the signature (+ – – –) in a single coordinate chart (t, r, θ, φ):

I $$ds_1^{(+)2} = \left(1 - \frac{r_b}{r} + \frac{r^2}{r_a^2}\right)c^2dt^2 - \frac{dr^2}{\left(1 - \frac{r_b}{r} + \frac{r^2}{r_a^2}\right)} - r^2d\theta^2 - r^2\sin^2\theta\, d\phi^2, \tag{9}$$

H $$ds_2^{(+)2} = \left(1 + \frac{r_b}{r} - \frac{r^2}{r_a^2}\right)c^2dt^2 - \frac{dr^2}{\left(1 + \frac{r_b}{r} - \frac{r^2}{r_a^2}\right)} - r^2d\theta^2 - r^2\sin^2\theta\, d\phi^2, \tag{10}$$

V $$ds_3^{(+)2} = \left(1 - \frac{r_b}{r} - \frac{r^2}{r_a^2}\right)c^2dt^2 - \frac{dr^2}{\left(1 - \frac{r_b}{r} - \frac{r^2}{r_a^2}\right)} - r^2d\theta^2 - r^2\sin^2\theta\, d\phi^2, \tag{11}$$

H′ $$ds_4^{(+)2} = \left(1 + \frac{r_b}{r} + \frac{r^2}{r_a^2}\right)c^2dt^2 - \frac{dr^2}{\left(1 + \frac{r_b}{r} + \frac{r^2}{r_a^2}\right)} - r^2d\theta^2 - r^2\sin^2\theta\, d\phi^2, \tag{12}$$

i $$ds_5^{(+)2} = c^2dt^2 - dr^2 - r^2d\theta^2 - r^2\sin^2\theta\, d\phi^2; \tag{13}$$

and five analogous metric solutions have the opposite signature (– + + +) in an analogous chart

H′ $$ds_1^{(-)2} = -\left(1 - \frac{r_b}{r} + \frac{r^2}{r_a^2}\right)c^2dt^2 + \frac{dr^2}{\left(1 - \frac{r_b}{r} + \frac{r^2}{r_a^2}\right)} + r^2d\theta^2 + r^2\sin^2\theta\, d\phi^2, \tag{14}$$

V $$ds_2^{(-)2} = -\left(1 + \frac{r_b}{r} - \frac{r^2}{r_a^2}\right)c^2dt^2 + \frac{dr^2}{\left(1 + \frac{r_b}{r} - \frac{r^2}{r_a^2}\right)} + r^2d\theta^2 + r^2\sin^2\theta\, d\phi^2, \tag{15}$$

H $$ds_3^{(-)2} = -\left(1 - \frac{r_b}{r} - \frac{r^2}{r_a^2}\right)c^2dt^2 + \frac{dr^2}{\left(1 - \frac{r_b}{r} - \frac{r^2}{r_a^2}\right)} + r^2d\theta^2 + r^2\sin^2\theta\, d\phi^2, \tag{16}$$

I $$ds_4^{(-)2} = -\left(1 + \frac{r_b}{r} + \frac{r^2}{r_a^2}\right)c^2dt^2 + \frac{dr^2}{\left(1 + \frac{r_b}{r} + \frac{r^2}{r_a^2}\right)} + r^2d\theta^2 + r^2\sin^2\theta\, d\phi^2, \tag{17}$$

i $$ds_5^{(-)2} = -\,c^2dt^2 + dr^2 + r^2(d\theta^2 + \sin^2\theta\, d\phi^2), \tag{18}$$

where r_b is the Schwarzschild radius.

**The generalized Birkhoff theorem states that any spherically symmetric solution of equation (7) with a non-constant areal radius is locally isometric to one of the solutions of the Kottler family (9)–(18); the exceptional case of a constant areal radius leads to the Nariai spacetime [24], which is not considered here.*

It is generally accepted that metrics with the signatures (+ – – –) and (– + + +), other things being equal, describe the same spacetime in different notation. Therefore, modern scientific works usually use only one of these signatures.

Moreover, metric solutions such as (9)–(13) are mostly considered separately for various cosmological problems (see Table 1).

Table 1. Metric solutions of the vacuum equation (7) for the signature (+ – – –)

No.	$f(r)$	Metric, Λ†
1	$1 - r_b/r + r^2/r_a^2$	$\Lambda > 0$ Schwarzschild–anti-de Sitter (Sch-AdS)
2	$1 + r_b/r - r^2/r_a^2$	$\Lambda < 0$ anti-Schwarzschild–de Sitter (ASch-dS)
3	$1 - r_b/r - r^2/r_a^2$	$\Lambda < 0$ Kottler–Schwarzschild–de Sitter** (standard Kott-Sch-dS metric)
4	$1 + r_b/r + r^2/r_a^2$	$\Lambda > 0$ anti-Schwarzschild–anti-de Sitter (ASch-AdS) (repulsive central solution)
5	1	$\Lambda = 0$ Minkowski (flat Minkowski spacetime)

†The sign of Λ refers to Eq. (1) with the Ricci tensor (2) and signature (+ – – –); in the convention most common in the literature, de Sitter-type solutions correspond to $\Lambda > 0$.

*** Kottler first wrote down a metric of the form (11) in [3], published in March 1918. In the limiting case $r_a \neq \infty$ and $r_b = 0$, the Kottler metric (11) becomes the de Sitter metric. In the opposite limit, $r_a = \infty$ and $r_b \neq 0$, it becomes the Schwarzschild metric. When both $r_a = \infty$ and $r_b = 0$, metrics (9)–(12) reduce to the Minkowski metric of flat spacetime. For this reason, the metric solutions (9)–(12) are usually called Schwarzschild–de Sitter and Schwarzschild–anti-de Sitter metrics (abbreviated Sch-dS and Sch-AdS).*

This article attempts to unify the metric solutions of the Kottler family (9)–(18) within a single system. To this end, we consider several possible ways of such unification.

3 Asymptotic Zero Metrics

Summing all 10 metric solutions (9)–(18) in a single coordinate chart

$$ds_0^{(\pm)2} = \sum_{i=1}^{5} ds_i^{(+)2} + \sum_{j=1}^{5} ds_j^{(-)2} = 0 \qquad (19)$$

is not an admissible operation because of the nonlinearity of equation (7), but it leads to two zero metrics with the total signature (+ – – –) + (– + + +) = (0 0 0 0):

$$ds_0^{(\pm)2} = \pm 0 \cdot c^2 dt^2 \mp 0 \cdot dr^2 \mp 0 \cdot r^2 d\theta^2 \mp 0 \cdot r^2 \, sin^2\,\theta \, d\phi^2 = 0. \qquad (20)$$

It is well established that the zero metrics (20) are not solutions of equation (7), since the Christoffel symbols (3) are undefined in this case

$$\lim_{g_{fl}\to 0} \Gamma_{ik}^{\lambda} = \lim_{g_{fl}\to 0} \left[\frac{1}{2} g^{\lambda\mu} \left(\frac{\partial g_{\mu k}}{\partial x^i} + \frac{\partial g_{i\mu}}{\partial x^k} - \frac{\partial g_{ik}}{\partial x^\mu}\right)\right] \to \frac{0}{0} = 0 \cdot \infty, \text{ where the indices } f \text{ and } l \text{ run over all values } \lambda, \mu, i, k,$$

since the expression $g^{\lambda\mu} = 1/g_{i\mu} = 1/0$ is incorrect. Moreover, the inverse metric $g^{\lambda\mu}$ *is* the inverse of the matrix $g_{i\mu}$, not an element-wise division followed by the limit *"1/0 → ∞"*.

However, it is not ruled out that in some cases the Ricci tensor (2) may turn out to be zero if, under certain conditions, the indeterminacies cancel each other through their differences:

$$\lim_{g_{fl}\to 0} R_{ik} = \lim_{g_{fl}\to 0} \left[\frac{\partial \Gamma_{ik}^l}{\partial x^l} - \frac{\partial \Gamma_{il}^l}{\partial x^k} + \Gamma_{ik}^l \Gamma_{lm}^m - \Gamma_{il}^m \Gamma_{mk}^l\right] \to \left[\frac{\partial(0\cdot\infty)}{\partial x^l} - \frac{\partial(0\cdot\infty)}{\partial x^k} + (0\cdot\infty)^2 - (0\cdot\infty)^2\right] \to [0+0] = 0.$$

We propose returning to this important limiting case, for example, by considering the degenerate limit of a one-parameter family $g_{i\mu}(\varepsilon)$ with a controlled limit $\varepsilon \to 0$, for which $R_{i\mu}(\varepsilon)$ is computed explicitly. This is beyond the scope of this article, but resolving this problem would make it possible to introduce a zero signature (i.e., a neutral element) into the group of the Algebra of Signatures under addition [16,17].

4 Problems of Unifying the Metric Solutions of the Vacuum Equation

Equation (7) determines the metric-dynamic state of a certain region of spacetime (i.e., of the Einstein vacuum), and it is not ruled out that all of its Lorentzian metric solutions (9)–(13) and (14)–(18) in a single coordinate chart are interrelated. The question arises: is it possible to unify these solutions within a single system?

Because of the nonlinearity of equation (7), the sums and differences of the metric solutions (9)–(18) are not solutions of this equation, except, possibly, for zero operations of type (19) (which require proof).

At the same time, one may assume that each metric solution of equation (7) belongs to a common system with a certain probability. In this case, one may attempt to apply an averaging operation.

As shown in the previous section, averaging all 10 metrics (9)–(18) leads to the zero result (20), while metrics (13) and (18) characterize not a curved state but the initial state of the vacuum (i.e., *flat Minkowski spacetime*). Therefore, we propose averaging metrics (9)–(12) and (14)–(17) separately, since they are defined in the same chart and have the same areal radius *r*.

However, averaging metrics is one of the most difficult problems in general relativity, known as the Isaacson–Buchert "averaging problem," on which an extensive literature exists, in particular [21–23,26,27]. The main question is: how can tensors be averaged while preserving their transformation law under a change of coordinates? There is still no general answer.

Reviews on this topic point out that there is currently no simple procedure for averaging vector and tensor quantities in general relativity. The point is that averaging metric components is tied to the chosen coordinates. If one changes coordinates, averages the transformed components, and compares the result with the previous result of averaging the components of the original metric, the results do not coincide. Averaging and coordinate transformation do not commute.

Zalaletdinov, Buchert, Green, and Wald showed in papers [21–23] that averaging the components of the metric tensor over a region of spacetime is a non-invariant operation, whereas averaging curvature invariants and scalars associated with these metrics is permissible.

Here we face a related problem: if, for example, we perform component-wise averaging of the ensembles of four metrics (9)–(12) or (14)–(17), we obtain, respectively, the averaged metrics

$$\langle ds_{\Sigma}^{(\pm)2}\rangle = \frac{1}{4}\sum_{i=1}^{4} ds_i^{(\pm)2} = \pm c^2dt^2 \mp \langle g_{rr}^{(\pm)}\rangle dr^2 \mp r^2 d\theta^2 \mp r^2 \sin^2\theta\, d\phi^2, \tag{21}$$

where $$\langle g_{rr}^{(\pm)}\rangle = \frac{1}{4}\left[\frac{1}{\left(1-\frac{r_b}{r}+\frac{r^2}{r_a^2}\right)} + \frac{1}{\left(1+\frac{r_b}{r}-\frac{r^2}{r_a^2}\right)} + \frac{1}{\left(1-\frac{r_b}{r}-\frac{r^2}{r_a^2}\right)} + \frac{1}{\left(1+\frac{r_b}{r}+\frac{r^2}{r_a^2}\right)}\right]. \tag{22}$$

These metrics are not solutions of the vacuum equation (7). For a finite ensemble of metrics given on the same manifold with a fixed identification of points, the pointwise average is itself a tensor; the actual difficulty lies in the non-uniqueness of this identification between different solutions (in the present model, this identification is fixed by adopting the same Kottler chart for all members of the ensemble, with the areal radius and the normalization of the static Killing field fixed in common) and in averaging over extended regions of spacetime [21–23].

5 Ways to Solve the "Averaging Problem" for Lorentzian Metrics

Let us consider several possible ways of solving the "averaging problem" for the Kottler family of Lorentzian metric solutions (9)–(18) of the vacuum equation (7).

5.1 Non-Invariant Averaging (Continuous-Medium Hypothesis)

Let us introduce an axiomatic prohibition on transitions from the spherical coordinate system (t, r, θ, φ) to other systems. This means that the region of vacuum under study is observed only from outside. In this case, the averaged geodesic lines are rigidly tied to the averaged extent of the elastoplastic vacuum and follow its deformations, like the bending of lines drawn on the surface of a bent rubber sheet.

In this case, it is permissible to consider the average metric (21), but the hypothesis then ceases to be relativistically invariant and belongs rather to continuum mechanics, using the parameters and mathematical apparatus of general relativity.

Let us substitute the components $\langle g_{ii}^{(+)}\rangle$ from the averaged metrics (21) into the expressions for the components of the 4-vector of relative elongation of the vacuum [15]

$$l_i^{(\pm)} = \sqrt{1+\frac{g_{ii}^{(\pm)}-g_{ii0}^{(\pm)}}{g_{ii0}^{(\pm)}}} - 1, \tag{23}$$

where the components $g_{ii0}^{(+)}$ and $g_{ii0}^{(-)}$ are taken, respectively, from the flat (initial) metrics (13) and (18). As a result, we obtain

$$l_r^{(\pm)} = \frac{\Delta r}{r} = \sqrt{1 + \frac{\langle g_{rr}^{(\pm)} \rangle - g_{rr0}^{(\pm)}}{g_{rr0}^{(\pm)}}} - 1 = \sqrt{\langle g_{11}^{(\pm)} \rangle} - 1 =$$

$$= \sqrt{\frac{1}{4}\left[\frac{1}{\left(1-\frac{r_b}{r}+\frac{r^2}{r_a^2}\right)} + \frac{1}{\left(1+\frac{r_b}{r}-\frac{r^2}{r_a^2}\right)} + \frac{1}{\left(1-\frac{r_b}{r}-\frac{r^2}{r_a^2}\right)} + \frac{1}{\left(1+\frac{r_b}{r}+\frac{r^2}{r_a^2}\right)}\right]} - 1 = \sqrt{\frac{1-\left(\frac{r_b}{r}\right)^2-\left(\frac{r^2}{r_a^2}\right)^2}{\left(1-\left(\frac{r_b}{r}+\frac{r^2}{r_a^2}\right)^2\right)\left(1-\left(\frac{r_b}{r}-\frac{r^2}{r_a^2}\right)^2\right)}} - 1, \qquad (24)$$

$$l_t^{(\pm)} = 0, \qquad l_\theta^{(\pm)} = 0, \qquad l_\phi^{(\pm)} = 0.$$

The function $l_r^{(\pm)}$ (24) shows the averaged relative elongation of the elastoplastic vacuum in the radial direction on the open interval between the inner and outer horizons, roughly $r_b < r < r_a$ (r_a and r_b have the dimension of length (meters); since equation (7) keeps its form when the metric is multiplied by a constant factor C^2 and Λ is divided by C^2, they may be of any scale). For the values $r_a = 90\ m$ and $r_b = 1.5$ m, conventionally adopted for illustration, the graph of function (24) diverges at the Schwarzschild horizon near $r \approx r_b$ and at the de Sitter horizon near $r \approx r_a$, so this function is defined on the interval $r \in (1.5004; 89.2404)$ (see Fig. 1*a*).

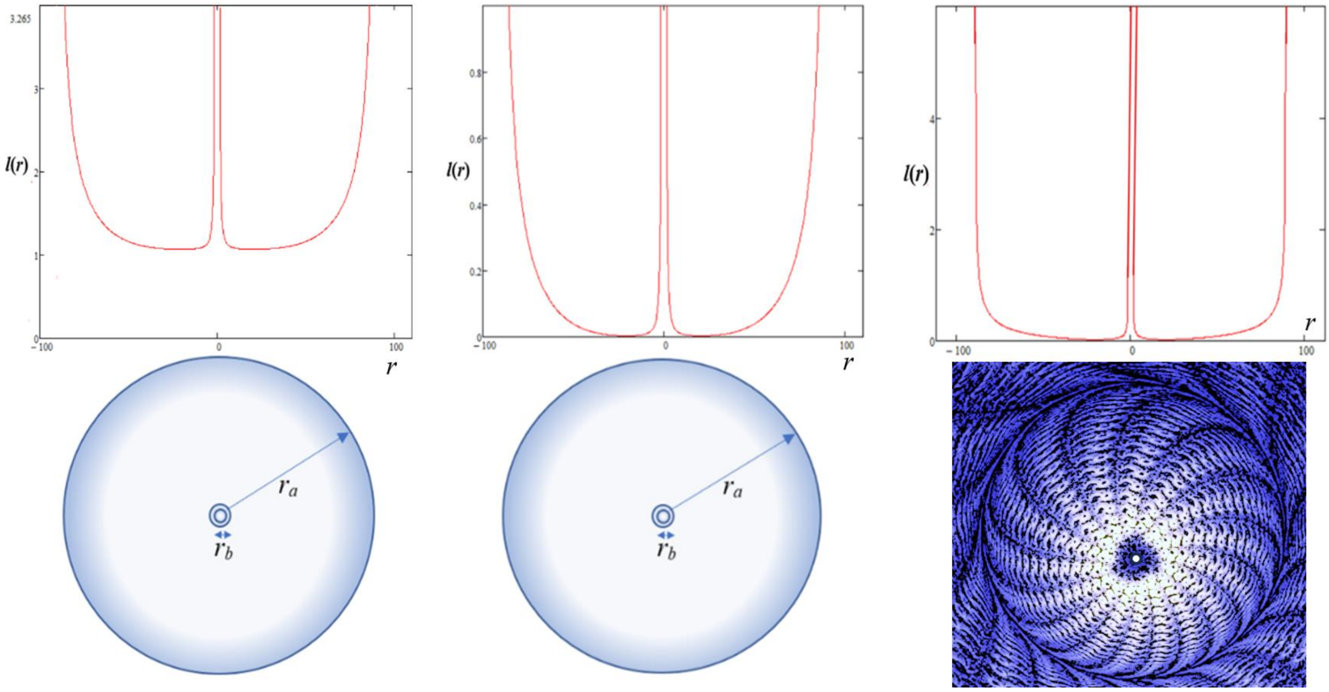

a) *b)* *c)*

Fig. 1: *Graphs of the relative elongation functions (illustrative): a) $l_r^{(\pm)}$ (24); b) $l_r^{(\pm)}$ (25); c) RMS($l_{rf}^{(\pm)}$) (32), for the conventionally adopted de Sitter radius $r_a = 90\ m$ and Schwarzschild radius $r_b = 1.5\ m$. The functions $l_r^{(+)}$ and RMS($l_{rf}^{(\pm)}$) determine the radial relative elongation of spacetime (i.e., of the Einstein vacuum) averaged over the ensembles of Lorentzian metrics (9)–(12) and (14)–(17). The common analytical domain of all three graphs is the interval between the inner and outer horizons, approximately 1.5004 < r < 89.2404 for the adopted values (roughly $r_b < r < r_a$); the left halves of the graphs are their mirror images, added for easier perception of the spherical objects. The calculations were performed using Mathcad. The lower part of Fig. 1c is not the result of a calculation based on formulas, but an artistic illustration using fractal images taken from open Internet sources.*

5.2 Invariant Arithmetic Averaging

As proposed in [21–23], we shall separately average the curvature invariants and scalars associated with the ensembles of metric solutions (9)–(12) and (14)–(17).

For example, the radial component of expression (23), $l_{ri}^{(\pm)} = \frac{\Delta r}{r} = \sqrt{g_{11i}^{(\pm)}} - 1$, is the ratio of the proper radial length to the differential of the areal radius, i.e., in this coordinate form a chart-dependent quantity rather than a curvature invariant; it can, however, be written as a true scalar*. The areal radius r is geometric; the decomposition into "proper radial length" is not unique if the four metrics (9)–(12) or (14)–(17) are allowed to have different $f(r)$. Therefore, we postulate that all four metrics are defined on the same coordinate chart. Then the angular part is the same, $r^2d\Omega^2$, in all four metrics (9)–(12) and all four metrics (14)–(17), so r means the same thing everywhere and is defined geometrically through the area of the sphere $A = 4\pi r^2$. In this case, the quantities subject to averaging are the invariant quantities (23), computed separately for each metric of the ensemble (9)–(12) and of the ensemble (14)–(17)**:

$$\langle l_r^{(\pm)}\rangle = \frac{1}{4}\left[\left(\sqrt{\frac{1}{\left(1-\frac{r_b}{r}+\frac{r^2}{r_a^2}\right)}}-1\right)+\left(\sqrt{\frac{1}{\left(1+\frac{r_b}{r}-\frac{r^2}{r_a^2}\right)}}-1\right)+\left(\sqrt{\frac{1}{\left(1-\frac{r_b}{r}-\frac{r^2}{r_a^2}\right)}}-1\right)+\left(\sqrt{\frac{1}{\left(1+\frac{r_b}{r}+\frac{r^2}{r_a^2}\right)}}-1\right)\right], \tag{25}$$

$$l_t^{(\pm)} = 0, \qquad l_\theta^{(\pm)} = 0, \qquad l_\phi^{(\pm)} = 0. \tag{26}$$

**Let R_A denote the areal radius, defined geometrically by the area $4\pi R_A^2$ of the orbits of spherical symmetry. For each metric $g_{(i)}$, we define the scalar $X_i = |g_{(i)}^{\mu\nu}\,\partial_\mu R_A\,\partial_\nu R_A|$ and $l_{ri} = X_i^{-1/2} - 1$. In the coordinates of (9)–(12), $R_A = r$, and on the domain considered here, where $f_i(r) > 0$, $X_i = f_i(r)$, so $l_{ri} = 1/\sqrt{f_i} - 1$, which reproduces (25); at the same time, l_{ri} is a true scalar, independent of the choice of coordinates.*

****In this article, we also postulate that each of the four metrics of the ensembles (9)–(12) and (14)–(17) participates in the common system with the same weight ¼. However, this does not follow from equation (7); therefore, expression (25) is the unweighted arithmetic mean over four Lorentzian metrics defined on the same chart.***

The results of calculations using formula (25), which are identical for the ensembles of metrics (9)–(12) and (14)–(17), are shown in Fig. 1*b*. For the conventionally adopted values $r_a = 90$ m and $r_b = 1.5$ m, the graph of function (25) tends to infinity near the horizons $r \approx r_b$ and $r \approx r_a$, so it is defined on the interval $r \in (1.5004; 89.2404)$.

In this case, the axiomatic prohibition on changing the reference frame can be lifted. This is an argument in favor of this approach, since the averaging results remain invariant.

Clearly, the results of formulas (24) and (25) differ; that is, averaging the components of metric tensors and averaging scalars do not give the same result.

The complete list of all scalars and polynomial curvature invariants of the metric solutions is practically infinite. Below we give the standard independent basis of scalars and invariants up to second order in curvature for the ensemble of metrics (9)–(12) (Table 2) and for the ensemble of metrics (14)–(17) (Table 3).

Table 2. Scalars and curvature invariants of the ensemble of metrics (9)–(12) with signature (+ – – –)

Squared interval	Killing vector norm $\xi_\mu\xi^\mu = g_{00}$	Kretschmann scalar, $K = R_{\mu\nu\rho\sigma}R^{\mu\nu\rho\sigma}$	Time component of the Ricci tensor*, R_{00}	Scalar curvature, $R=4\Lambda$	Weyl invariant $C_{\mu\nu\rho\sigma}C^{\mu\nu\rho\sigma}$	$R^0{}_0 = g^{00}R_{00}$	Squared Ricci tensor $R_{\mu\nu}R^{\mu\nu}$
$ds_1^{(+)2}$	$1-\frac{r_b}{r}+\frac{r^2}{r_a^2}$	$\frac{12r_b^2}{r^6}+\frac{24}{r_a^4}$	$\frac{3c^2}{r_a^2}\left(1-\frac{r_b}{r}+\frac{r^2}{r_a^2}\right)$	$+12/r_a^2$	$\frac{12\,r_b^2}{r^6}$	$+\frac{3}{r_a^2}$	$\frac{36}{r_a^4}$
$ds_2^{(+)2}$	$1+\frac{r_b}{r}-\frac{r^2}{r_a^2}$	$\frac{12r_b^2}{r^6}+\frac{24}{r_a^4}$	$-\frac{3c^2}{r_a^2}\left(1+\frac{r_b}{r}-\frac{r^2}{r_a^2}\right)$	$-12/r_a^2$	$\frac{12\,r_b^2}{r^6}$	$-\frac{3}{r_a^2}$	$\frac{36}{r_a^4}$
$ds_3^{(+)2}$	$1-\frac{r_b}{r}-\frac{r^2}{r_a^2}$	$\frac{12r_b^2}{r^6}+\frac{24}{r_a^4}$	$-\frac{3c^2}{r_a^2}\left(1-\frac{r_b}{r}-\frac{r^2}{r_a^2}\right)$	$-12/r_a^2$	$\frac{12\,r_b^2}{r^6}$	$-\frac{3}{r_a^2}$	$\frac{36}{r_a^4}$
$ds_4^{(+)2}$	$1+\frac{r_b}{r}+\frac{r^2}{r_a^2}$	$\frac{12r_b^2}{r^6}+\frac{24}{r_a^4}$	$\frac{3c^2}{r_a^2}\left(1+\frac{r_b}{r}+\frac{r^2}{r_a^2}\right)$	$+12/r_a^2$	$\frac{12\,r_b^2}{r^6}$	$+\frac{3}{r_a^2}$	$\frac{36}{r_a^4}$

**Here R_{00} denotes the scalar $R_{\mu\nu}\xi^\mu\xi^\nu$ for the static Killing field $\xi = \partial_t$, with the normalization of ξ fixed by the common Kottler chart used throughout this paper; strictly speaking, it is a scalar associated with the Killing field rather than a curvature invariant.*

Table 3. Scalars and curvature invariants of the ensemble of metrics (14)–(17) with signature (– + + +)

Squared interval	Killing vector norm $\xi_\mu\xi^\mu = g_{00}$	Kretschmann scalar, $K = R_{\mu\nu\rho\sigma}R^{\mu\nu\rho\sigma}$	Time component of the Ricci tensor, R_{00}	Scalar curvature, R=4Λ	Weyl invariant $C_{\mu\nu\rho\sigma}C^{\mu\nu\rho\sigma}$	$R^0_{\ 0} = g^{00}R_{00}$	Squared Ricci tensor $R_{\mu\nu}R^{\mu\nu}$
$ds_1^{(-)2}$	$-\left(1-\frac{r_b}{r}+\frac{r^2}{r_a^2}\right)$	$\frac{12r_b^2}{r^6}+\frac{24}{r_a^4}$	$\frac{3c^2}{r_a^2}\left(1-\frac{r_b}{r}+\frac{r^2}{r_a^2}\right)$	$-12/r_a^2$	$\frac{12\,r_b^2}{r^6}$	$-\frac{3}{r_a^2}$	$\frac{36}{r_a^4}$
$ds_2^{(-)2}$	$-\left(1+\frac{r_b}{r}-\frac{r^2}{r_a^2}\right)$	$\frac{12r_b^2}{r^6}+\frac{24}{r_a^4}$	$-\frac{3c^2}{r_a^2}\left(1+\frac{r_b}{r}-\frac{r^2}{r_a^2}\right)$	$+12/r_a^2$	$\frac{12\,r_b^2}{r^6}$	$+\frac{3}{r_a^2}$	$\frac{36}{r_a^4}$
$ds_3^{(-)2}$	$-\left(1-\frac{r_b}{r}-\frac{r^2}{r_a^2}\right)$	$\frac{12r_b^2}{r^6}+\frac{24}{r_a^4}$	$-\frac{3c^2}{r_a^2}\left(1-\frac{r_b}{r}-\frac{r^2}{r_a^2}\right)$	$+12/r_a^2$	$\frac{12\,r_b^2}{r^6}$	$+\frac{3}{r_a^2}$	$\frac{36}{r_a^4}$
$ds_4^{(-)2}$	$-\left(1+\frac{r_b}{r}+\frac{r^2}{r_a^2}\right)$	$\frac{12r_b^2}{r^6}+\frac{24}{r_a^4}$	$\frac{3c^2}{r_a^2}\left(1+\frac{r_b}{r}+\frac{r^2}{r_a^2}\right)$	$-12/r_a^2$	$\frac{12\,r_b^2}{r^6}$	$-\frac{3}{r_a^2}$	$\frac{36}{r_a^4}$

A comparison of Tables 2 and 3 shows that some scalars and invariants for metrics with the different signatures (+ – – –) and (– + + +) coincide only up to sign, for example, $\xi_\mu\xi^\mu$, R and $R^0_{\ 0}$. Within the present model, we adopt the distinction between these two sign-related branches as an additional hypothesis: the metric solutions (9)–(12) and (14)–(17), which have mutually opposite signatures, describe different objects. In addition, it was shown in [17,18] that metric spaces with the mutually opposite signatures (+ – – –) and (– + + +) are rotated relative to each other by 90°.

Note also that such curvature scalars and invariants as the total curvature (i.e., the Kretschmann scalar) $K = R_{\mu\nu\rho\sigma}R^{\mu\nu\rho\sigma}$, the Weyl invariant $C_{\mu\nu\rho\sigma}C^{\mu\nu\rho\sigma}$ and the squared Ricci tensor $R_{\mu\nu}R^{\mu\nu}$ are the same for all metric solutions (9)–(12) and (14)–(17).

Under the equal-weight (¼) hypothesis, the arithmetic mean of the scalars and curvature invariants of the Lorentzian metrics (9)–(12) (from Table 2) almost completely coincides with the arithmetic mean of the scalars and curvature invariants of metrics (14)–(17) (from Table 3); see Table 4.

Table 4. Mean scalars and curvature invariants of the ensembles of metrics (9)–(12) and (14)–(17)

Mean (interval)^2	Killing vector norm $\langle\xi_\mu\xi^\mu\rangle = \langle g_{00}\rangle$	Kretschmann scalar, $\langle K\rangle = \langle R_{\mu\nu\rho\sigma}R^{\mu\nu\rho\sigma}\rangle$	Time component of the Ricci tensor, $\langle R_{00}\rangle$	Scalar curvature, $\langle R\rangle$=$\langle 4\Lambda\rangle$	Weyl invariant $\langle C_{\mu\nu\rho\sigma}C^{\mu\nu\rho\sigma}\rangle$	$\langle R^0_{\ 0}\rangle = \langle g^{00}R_{00}\rangle$	Squared Ricci tensor $\langle R_{\mu\nu}R^{\mu\nu}\rangle$
$\langle ds_i^{(\pm)2}\rangle$	±1 + for (+ – – –) – for (– + + +)	$\frac{12r_b^2}{r^6}+\frac{24}{r_a^4}$	$\frac{3c^2r^2}{r_a^4}$	0	$\frac{12\,r_b^2}{r^6}$	0	$\frac{36}{r_a^4}$

The averaged scalars and curvature invariants of the ensembles of metrics (9)–(12) and (14)–(17) presented in Table 4 are quantities that do not change under a change of coordinate system; therefore, they reflect the intrinsic geometric properties of the curved region of the averaged vacuum under study, with the averaged relative elongations (25) (Fig. 1*b*).

Let us note the following feature. The norms of the Killing vector $\xi_\mu\xi^\mu$ for metrics (9)–(12) and (14)–(17) are equal to their zeroth (i.e., time) components (see Tables 2 and 3). These norms, as is well known, are scalar functions of *r*. They depend on the radial coordinate, but the values of $\xi_\mu\xi^\mu$ themselves are scalars at each point of the region under study for a fixed Killing field ξ_μ. In this case, averaging the scalars $\xi_\mu\xi^\mu$ is an invariant operation, giving $\langle g_{00}\rangle = \langle g_{tt}^{(\pm)}\rangle = \pm1$. Thus, in this chart, within the admissible domain of function (25), on average over the ensembles of solutions (9)–(12) and (14)–(17), the gravitational time dilation (i.e., the averaged redshift factor) cancels out.

5.3 Invariant Root-Mean-Square Averaging (Fabric Hypothesis)

Let us consider one more invariant way of combining the family of metric solutions of the vacuum equation (7) into a unified spacetime system.

The Lorentzian intervals $ds_i^{(+)2}$ (9)–(12) and $ds_i^{(-)2}(14) - (17)$ are scalars for a given displacement dx^i; therefore, their averaging is an invariant operation:

$$\langle s_{1-4}^{(+)2}\rangle = \frac{1}{4}\left(ds_1^{(+)2} + ds_2^{(+)2} + ds_3^{(+)2} + ds_4^{(+)2}\right), \tag{27}$$

$$\langle s_{1-4}^{(-)2}\rangle = \frac{1}{4}\left(ds_1^{(-)2} + ds_2^{(-)2} + ds_3^{(-)2} + ds_4^{(-)2}\right). \tag{28}$$

Expressions (27) and (28) can be represented as the scalar product of complex-conjugate half-quaternions (i.e., quaternions divided by 2) [17,18]

$$\langle s_{1-4}^{(\pm)2}\rangle = \frac{1}{2}\left(ds_1^{(\pm)} + i ds_2^{(\pm)} + j ds_3^{(\pm)} + k\, ds_4^{(\pm)}\right)\frac{1}{2}\left(ds_1^{(\pm)} - i ds_2^{(\pm)} - j ds_3^{(\pm)} - k\, ds_4^{(\pm)}\right), \tag{29}$$

where $ds_i^{(\pm)}$ are absolute invariants;

i, j, k are the imaginary units that form an orthonormal basis of the algebra of quaternions H, which is isomorphic to the even Clifford subalgebra Cl⁰(3)

$$i^2 = j^2 = k^2 = ijk = -1,\ ij = -ji = k, \quad jk = -kj = i,\ ki = -ik = j. \tag{30}$$

The properties of quaternions suggest, and we adopt this as a modeling assumption, that the conventionally "colored" segments of lines (i.e., "colored threads") $ds_1^{(\pm)}, ds_2^{(\pm)}, ds_3^{(\pm)}, ds_4^{(\pm)}$ are everywhere mutually perpendicular: $ds_1^{(\pm)} \perp ds_2^{(\pm)} \perp ds_3^{(\pm)} \perp ds_4^{(\pm)}$. This is possible if the "colored" invariant threads $s_1^{(\pm)},\ s_2^{(\pm)},\ s_3^{(\pm)},\ s_4^{(\pm)}$ (where $s_{nd}^{(\pm)} = \sqrt{g_{ikd}^{(\pm)}\, dx^i dx^k}$, d = 1, 2, 3, 4) are interwoven into 4-strand helices that form an elastoplastic vacuum fabric [16,17,18,19] (see the fractal illustrations in Fig. 1*c*).

Representing the vacuum conventionally as a flexible elastoplastic fabric entails the following consequences. The averaged relative elongations for the ensembles of metrics (9)–(12) and (14)–(17) take the form of half-quaternions (i.e., quaternions divided by 2)

$$l_{rf}^{(\pm)} = \left[\frac{1}{2}\left(\sqrt{\frac{1}{\left(1-\frac{r_b}{r}+\frac{r^2}{r_a^2}\right)}}-1\right) + i\frac{1}{2}\left(\sqrt{\frac{1}{\left(1+\frac{r_b}{r}-\frac{r^2}{r_a^2}\right)}}-1\right) + j\frac{1}{2}\left(\sqrt{\frac{1}{\left(1-\frac{r_b}{r}-\frac{r^2}{r_a^2}\right)}}-1\right) + k\frac{1}{2}\left(\sqrt{\frac{1}{\left(1+\frac{r_b}{r}+\frac{r^2}{r_a^2}\right)}}-1\right)\right], \tag{31}$$

and the corresponding scalars may be the moduli of these quaternions, which in this case coincide with the root-mean-square values

$$\left|l_{rf}^{(\pm)}\right| = \mathrm{RMS}(l_{rf}^{(\pm)}) = \frac{1}{2}\sqrt{\left(\sqrt{\frac{1}{\left(1-\frac{r_b}{r}+\frac{r^2}{r_a^2}\right)}}-1\right)^2 + \left(\sqrt{\frac{1}{\left(1+\frac{r_b}{r}-\frac{r^2}{r_a^2}\right)}}-1\right)^2 + \left(\sqrt{\frac{1}{\left(1-\frac{r_b}{r}-\frac{r^2}{r_a^2}\right)}}-1\right)^2 + \left(\sqrt{\frac{1}{\left(1+\frac{r_b}{r}+\frac{r^2}{r_a^2}\right)}}-1\right)^2}. \tag{32}$$

The graphs of functions (32) coincide for the conventionally adopted values $r_a = 90$ m and $r_b = 1.5$ m, and are shown in Fig. 1*c*. At the boundaries of the admissible interval $r \in (r_b \approx 1.5004;\ r_a \approx 89.2404)$ the functions (32) tend to infinity.

Using the data from Tables 2 and 3, we similarly calculate the root-mean-square (RMS) values of the scalars and curvature invariants of the ensembles of metrics (9)–(12) and (14)–(17) using the formula

$$\mathrm{RMS}(a) = \sqrt{\frac{a_1^2+a_2^2+a_3^2+a_4^2}{4}} = \frac{1}{2}\sqrt{a_1^2+a_2^2+a_3^2+a_4^2}.$$

The results are presented in Table 5.

Table 5. Identical root-mean-square curvature invariants of the ensembles of metrics (9)–(12) and (14)–(17)

RMS (interval)² $ds_1^{(+)2}$	RMS of the Killing vector norm $\xi_\mu\xi^\mu = g_{00}$	RMS of the Kretsch-mann scalar, $K = R_{\mu\nu\rho\sigma}R^{\mu\nu\rho\sigma}$	RMS of the time component of the Ricci tensor, R_{00}	RMS of the scalar curvature, $R=4\Lambda$	RMS of the Weyl invariant $C_{\mu\nu\rho\sigma}C^{\mu\nu\rho\sigma}$	RMS $R^0_{\ 0} = g^{00}R_{00}$	RMS of the squared Ricci tensor $R_{\mu\nu}R^{\mu\nu}$
$ds_\Sigma^{(+)2}$	$\sqrt{1+\frac{r_b^2}{r^2}+\frac{r^4}{r_a^4}}$	$\frac{12r_b^2}{r^6}+\frac{24}{r_a^4}$	$\frac{3c^2}{r_a^2}\sqrt{1+\frac{r_b^2}{r^2}+\frac{r^4}{r_a^4}}$	$\frac{12}{r_a^2}$	$\frac{12\,r_b^2}{r^6}$	$\frac{3}{r_a^2}$	$\frac{36}{r_a^4}$

Let us note once again that the root-mean-square scalars and curvature invariants of the ensembles of metrics (9)–(12) and (14)–(17) presented in Table 5 coincide completely.

Comparing the data in Tables 2, 3, and 5, we find that the following parameters coincide up to sign: RMS $(K) = K$, RMS $(R) = \pm R$, RMS $(R^0_{\ 0}) = \pm R^0_{\ 0}$ and RMS $(R_{\mu\nu}R^{\mu\nu}) = R_{\mu\nu}R^{\mu\nu}$.

The root-mean-square curvature invariants of the ensembles of metrics (9)–(12) and (14)–(17) presented in Table 5 are quantities that do not change under a change of coordinate system; therefore, they reflect the intrinsic geometric properties of the curved vacuum fabric under study, with the root-mean-square relative elongation (32) (Fig. 1c).

6 Kottler–Schwarzschild–de Sitter "Corpuscles" and "Anti-Corpuscles"

In modern theories based on general relativity, it is customary to regard the change of sign of some scalars under the signature change $(+---) \to (-+++)$ (compare Tables 2 and 3) as a standard consequence of a change of convention. However, in the author's opinion, one cannot categorically reject the hypothesis that the ensembles of Lorentzian metrics (9)–(12) and (14)–(17) with mutually opposite signatures define metric-dynamic models of two different, opposite objects.

Moreover, a two-dimensional example in § 5.2 of [18] demonstrates that if coordinate charts with opposite signatures are located on opposite sides of the sheet, they are rotated by 90° relative to each other.

Taken together, the above considerations show that the ensembles of metric solutions (9)–(12) and (14)–(17) of the Einstein vacuum equation (7) describe, on the one hand, identical and, on the other hand, mutually opposite closed spherical objects rotated relative to each other by 90° (however, owing to spherical symmetry, this rotation, or phase shift, between the objects is practically unnoticeable).

Taking into account the opposite signs of some scalars (Tables 2 and 3) and other properties, we have conventionally assumed that the ensemble of metrics (9)–(12) describes an averaged closed convexity* of spacetime (i.e., of the averaged Einstein vacuum), while the ensemble of metrics (14)–(17) describes the opposite averaged closed concavity* of the averaged vacuum.

**It is impossible to visualize a 3-dimensional (let alone a 4-dimensional) convexity or concavity of spacetime; here we attempt to synthesize a language for describing two opposite stable spherical curvatures of the multilayer Einstein vacuum on an auxiliary, figurative binary linguistic basis.*

From the graphs in Fig. 1b and 1c it can be seen that, with either invariant arithmetic or root-mean-square averaging over the ensemble of metrics (9)–(12) with signature $(+---)$, one obtains a model of an almost hollow ball resembling the static de Sitter world, with a strongly stretched periphery. Inside the large de Sitter ball there is a strongly stretched neighborhood of a small spherical cavity, which we shall call the Schwarzschild "nucleolus" (or "pit"). We conventionally call such a stable closed spherical vacuum formation a convex Kottler–Schwarzschild–de Sitter "corpuscle" (or "apple") (abbreviated as the *KSdS* "corpuscle")*.

**The divergence of the function* $\sqrt{(1/f)}-1$ *at the roots of f(r) = 0 corresponds to the horizons of each individual Kottler metric, not to the wall of the averaged corpuscle, and the results obtained are only a set of mean scalars on the interval between the inner and outer horizons (roughly* $r_b < r < r_a$*). Nevertheless, the object under study has a pronounced spherical shape and a spherical boundary. Therefore, the illustrative term "corpuscle" is appropriate for the averaged mathematical model.*

The ensemble of metric solutions (14)–(17) with the opposite signature $(-+++)$, in turn, makes it possible to construct an identically structured averaged, but antipodal, closed spherical concavity of the vacuum (i.e., the *KSdS* "anti-corpuscle").

The *KSdS* corpuscle with signature $(+---)$ and the *KSdS* anti-corpuscle with signature $(-+++)$ are called a spherical convexity and a spherical concavity of the vacuum, respectively, because they completely compensate each other's manifestations: $(+---) + (-+++) = (0\ 0\ 0\ 0)$, like a particle and an antiparticle.

The corpuscle woven from vacuum fabric (Figs. 1c and 2), with the root-mean-square relative elongation (32), differs from the on-average linearly deformed corpuscle (Fig. 1b) in that the woven corpuscle resembles a thin-walled soap bubble.

The radii r_b *and* r_a are initially undetermined. That is, since equation (7) keeps its form when the metric is multiplied by a constant factor C^2 and Λ is divided by C^2, solutions exist for any values of these radii under the condition $r_b \ll r_a$, more precisely, for $\frac{r_b}{r_a} < \frac{2}{3\sqrt{3}} \approx 0.3849$. Therefore, the above-mentioned *KSdS* corpuscle and *KSdS* anti-corpuscle can be of any size. This made it possible to develop the Hierarchical Cosmological Model [19,20], in which the world is filled with a vast multitude of corpuscles and anti-corpuscles of various scales with a discrete set of radii r_{ai} and r_{bj}.

7 Extended Einstein Vacuum Equation

In the previous sections, it was shown that the Einstein vacuum equation with a Λ-term (7) has the potential to describe one *KSdS* corpuscle (i.e., a closed spherical convexity of the vacuum) and one *KSdS* anti-corpuscle (i.e., a closed spherical concavity of the vacuum).

This leads to the following problems:

1) The scaling property of equation (7) (the metric multiplied by C^2, Λ divided by C^2) allows the *KSdS* corpuscle and the *KSdS* anti-corpuscle to be of any size, but there are only two of them. Where is the enormous diversity of the colossal number of corpuscles (i.e., particle cores) and anti-corpuscles (i.e., antiparticle cores)?

2) Within the model under consideration, based on the invariant averaging of scalars and curvature invariants of the ensembles of Lorentzian metric solutions (9)–(12) and (14)–(17) of the vacuum equation (7), it is impossible to describe the interaction between a *KSdS* corpuscle and a *KSdS* anti-corpuscle isolated from each other;

3) For the *KSdS* corpuscle and the *KSdS* anti-corpuscle, the averaged relative elongation tends to infinity at their spherical periphery and near the small central spherical cavity (Figs. 1*b* and 1*c*);

4) It is unclear what lies beyond the outer spherical de Sitter boundary of the *KSdS* corpuscle and the *KSdS* anti-corpuscle, and what lies inside their central Schwarzschild cavity. Within the mathematical model under consideration, there is nothing there, not even curved vacuum (Figs. 1*b* and 1*c*). This is unacceptable.

5) According to current understanding, metrics with the opposite signatures (+ – – –) and (– + + +) are interchangeable and describe the same manifold in different notation. Within such an axiomatic framework, the set of metrics (9)–(13) with signature (+ – – –) and the set of metrics (14)–(18) with signature (– + + +) describe the same spherical region of the vacuum. That is, there is a twofold degeneracy. However, there is a difference between them, in particular, the opposite signs of some invariants (see Tables 2 and 3). Moreover, this degeneracy splits into two mutually opposite objects rotated relative to each other by 90°.

This leads to the following dilemma. On the one hand, the Kottler family of metrics (9)–(18) is extremely significant, since it is an interrelated set of solutions of one of the most fundamental equations of modern physics, (7). On the other hand, the invariant averaging of the two mutually opposite ensembles of these metrics has led to the problems listed above. The vacuum equation (7) offers no way out of this situation.

In an attempt to solve these and many other problems, paper [19] proposed, as a hypothesis, an extended Einstein vacuum equation with a large number of positive and negative Λ-terms

$$R_{ik} - ½\, g_{ik}(\textstyle\sum_{m=1}^{M}\Lambda_m + \sum_{n=1}^{N} -\Lambda_n) = 0, \tag{33}$$

where $\Lambda_m = \frac{3}{r_m^2}$, $\Lambda_n = \frac{3}{r_n^2}$, here r_m is the core radius of the *m*th corpuscle, r_n is the core radius of the *n*th anti-corpuscle; M is the number of corpuscles, tending to ∞; N is the number of anti-corpuscles, tending to ∞.

Even if the radii r_m and r_n decrease toward small scales, the series $\sum_{m=1}^{M}\Lambda_m$ and $\sum_{n=1}^{N}\Lambda_n$ diverge (i.e., have no finite limit), but their difference may be finite. This makes it possible to impose on the extended Einstein vacuum equation (33) the condition*

$$½\,(\textstyle\sum_{m=1}^{M}\Lambda_m + \sum_{n=1}^{N} -\Lambda_n) = ½\,(\sum_{m=1}^{M}\Lambda_m - \sum_{n=1}^{N}\Lambda_n) = \Lambda_0 = constant. \tag{34}$$

**The difference in (34) is understood as the limit of the differences of partial sums under a specified common-cutoff prescription, provided that this limit exists; in the present model, the existence and value of this regularized limit are assumed as part of condition (34). Under this condition, Eq. (33) reduces to Eq. (7) with $\Lambda = \Lambda_0$, and its role is the decomposition of Λ_0 into contributions of individual corpuscles, which leads to the source interpretation (38)–(39).*

If $R_{ik} = \Lambda_0(x)g_{ik}$ holds on a connected manifold of dimension $n > 2$, the contracted Bianchi identity forces Λ_0 to be constant (Schur's lemma; cf. [25]); condition (34) is therefore consistent with the field equation rather than an additional assumption. Taking the trace gives the constant scalar curvature

$$R = g^{ik}R_{ik} = g^{ik}g_{ik}\Lambda_0 = n\Lambda_0 = 4\Lambda_0. \tag{35}$$

When condition (34) is satisfied, the extended vacuum equation (33) has the same properties as the Einstein vacuum equation (7), since in this case the covariant derivative of its left-hand side is also zero, similarly to expression (6):

$$\nabla_j[R_{ik} - ½\, g_{ik}(\textstyle\sum_{m=1}^{\infty}\Lambda_m + \sum_{n=1}^{\infty} -\Lambda_n)] = \nabla_j[R_{ik} - g_{ik}\Lambda_0] = 0. \tag{36}$$

The extended vacuum equation (33) opens up broad possibilities; for example, if this equation is written in the following form

$$R_{ik} - ½\, g_{ik}\big(\textstyle\sum_{h=1}^{H}\Lambda_h + \sum_{p=1}^{P} -\Lambda_p\big) - ½\, g_{ik}(\sum_{a=1}^{A}\Lambda_a + \sum_{b=1}^{B} -\Lambda_b) = 0, \tag{37}$$

where

$½\,\big(\sum_{h=1}^{H}\Lambda_h + \sum_{p=1}^{P} -\Lambda_p\big) = T_s$ for corpuscles and anti-corpuscles of the microworld,

(38)

$½\,(\sum_{a=1}^{A}\Lambda_a + \sum_{b=1}^{B} -\Lambda_b) = \Lambda_B$ for corpuscles and anti-corpuscles of the macroworld,

and $(\Lambda_B + T_s) = \Lambda_0$.

Then, taking into account the constancy of the scalar curvature (35), $R = 4\Lambda_0 = 4(\Lambda_B + T_s)$, equation (37) takes the form

$$R_{ik} - \Lambda_0 g_{ik} = R_{ik} - \tfrac{1}{2}R\, g_{ik} + \Lambda_0\, g_{ik} = R_{ik} - \tfrac{1}{2}R\, g_{ik} + (T_s + \Lambda_B)\, g_{ik} = 0.$$

As a result, we obtain an equation with sources (38):

$$R_{ik} - \frac{1}{2} R\, g_{ik} + \Lambda_B\, g_{ik} = -T_s\, g_{ik}, \tag{39}$$

which, for $\Lambda_B = 1.089 \cdot 10^{-52}$ m^{-2}, has the form of an equation suitable for discussing cosmological problems.

Moving the constant term $T_s\, g_{ik}$ to the right-hand side corresponds to the standard interpretation of part of the cosmological term as the vacuum energy–momentum tensor, proportional to g_{ik} [28, 29].

Conclusions

One may expect that different solutions of the same nonlinear differential equation with the same boundary conditions may be interrelated and may describe a single system.

Whenever we exclude certain solutions of the equations of mathematical physics from consideration, this ultimately and inevitably leads to dead ends, paradoxes, singularities, divergences, and other negative consequences. Conversely, taking into account all the possibilities provided by mathematics steadily leads to logically complete models.

The purpose of this paper is to show that taking into account all 10 possible Lorentzian metric solutions of the Kottler family (9)–(18) of the Einstein vacuum equation (7) within a single system leads to meaningful results.

The main difficulties in unifying these metrics into a single system are: 1) the generally accepted statement that the sum of solutions of a nonlinear equation is not a solution of that equation; and 2) the "averaging problem," which consists in the fact that averaging the components of the metric tensor g_{ik} over an extended region of spacetime is a non-invariant operation, while for an ensemble of metric solutions the result depends on how the points of different solutions are identified.

In this article, we propose to regard the metric solutions (9)–(18) in a single coordinate chart as being realized as parts of a unified system with a certain probability. In this case, referring to papers [21–23], we have replaced the component-wise adding and averaging of the metric tensor components of the solutions of equation (7) with the arithmetic and root-mean-square averaging of the scalars and curvature invariants associated with the ensembles of metrics (9)–(12) and (14)–(17) (see Tables 4 and 5). With this approach, the averaged scalars and curvature invariants correspond to regions of spacetime (i.e., of the Einstein vacuum) averaged over the ensembles of metrics.

The article considers four operations with the metric solutions of the Kottler family (9)–(18): 1) the formal zero sum of intervals (19); 2) the non-invariant component-wise mean (21); 3) the invariant arithmetic mean of scalars (25)–(26); and 4) the invariant half-quaternion RMS mean (29)–(32). We give preference to the fourth; however, the other operations require further detailed consideration.

As a result of the invariant averaging of the ensembles of metrics (9)–(12) with signature (+ – – –) and (14)–(17) with the opposite signature (– + + +), we obtained models of a stable spherically closed convexity of the vacuum and a stable spherically closed concavity of the vacuum, which we have conventionally called the *KSdS* corpuscle and the *KSdS* anti-corpuscle with the averaged relative elongations of the vacuum (25) or (32) (see Fig. 1*b* or 1*c*).

Since coordinate charts with opposite signatures – located on either side of the metric sheet – are perpendicular to each other, a corpuscle (particle) and an anti-corpuscle (antiparticle) are likewise rotated by 90° relative to one another (see the example of the two-sided case in §5.2 of [18]). It is possible that this phase shift underlies the explanation for the Sakharov conditions regarding the baryon asymmetry of matter.

The resulting models of the *KSdS* corpuscle and the *KSdS* anti-corpuscle have a number of shortcomings and problems, listed above; to solve them, paper [19] proposed the extended Einstein vacuum equation (EVE) with a large number of $\pm\Lambda_i$-terms (33):

$$R_{ik} - ½\, g_{ik}\left(\textstyle\sum_{m=1}^{M} \Lambda_m + \sum_{n=1}^{N} -\Lambda_n\right) = 0, \tag{33′}$$

which, taking into account all 16 ordered sign patterns of 4-dimensional metric spaces (signatures in the sense of the Algebra of Signatures [16,17])

$$sign(ds^2) = \begin{pmatrix} (++++) & (+++-) & (-++-) & (++-+) \\ (---+) & (-+++) & (--++) & (-+-+) \\ (+--+) & (++--) & (+---) & (+-++) \\ (--+-) & (+-+-) & (-+--) & (----) \end{pmatrix} \tag{40}$$

in our view, has the potential to outline paths for developing the Hierarchical Cosmological Model ("EVE project") [16 – 20], aimed at advancing the Clifford–Einstein–Wheeler program for the geometrization of many branches of physics.

Author contributions
The author did all the research work for this study.

Competing interests
The author has declared that no competing interests exist.

Data access statement
Materials are available on request.

Ethics statement
All ethical standards are observed. Links to articles by other researchers are provided.

Funding statement
This research received no external funding.

Acknowledgments

I sincerely thank David Reid, Tatiana Levi, Georgy Usachev, and Eugene Etingin for their help, and I am grateful to Gennady Shipov and Evgeny Guborev, Academicians of the Russian Academy of Natural Sciences, for fruitful discussions of the issues considered here.

Generative AI tools were used in the preparation of this manuscript: Claude Opus 5 (Anthropic) for translation from Russian into English, language editing, and suggested wording of several technical clarifications; GPT-5.6 Sol (OpenAI) for independent checking of the manuscript and of these clarifications. The author reviewed all AI-assisted content and takes full responsibility for the final text.

References

[1] Stephani, H.; Kramer, D.; MacCallum, M.; Hoenselaers, C.; Herlt, E. (2003). Exact Solutions of Einstein's Field Equations, 2nd ed. (Cambridge University Press, Cambridge).
[2] Griffiths, J. B. & Podolský, J. (2009). Exact Space-Times in Einstein's General Relativity (Cambridge University Press, Cambridge, UK).
[3] Kottler, F. (1918). Über die physikalischen Grundlagen der Einsteinschen Gravitationstheorie. Annalen der Physik, Vol. 56, pp. 401–462. doi:10.1002/andp.19183611402.
[4] Alexanian, M. (2026). Effective de Sitter-Schwarzschild Metrics. Armenian Journal of Physics, vol. 19, issue 2, pp. 107-112, arXiv:2607.09707.
[5] Shen, M. & Zhuang, O. (2016). A New Class of Solutions of Vacuum Einstein's Field Equations with Cosmological Constant. Annals of Applied Mathematics, Vol. 32, No. 1, pp. 36 – 41.
[6] Cha, Ye Sle, & Marcus Khuri (2018). Transformations of asymptotically AdS hyperbolic initial data and associated geometric inequalities. General Relativity and Gravitation 50.1: 3.
[7] Chruściel, Piotr T., Daniel Maerten, and Paul Tod (2006). Rigid upper bounds for the angular momentum and center of mass of non-singular asymptotically anti-de Sitter space-times. Journal of High Energy Physics 2006.11: 084-084.
[8] Ashraf Azman, M. (2026). Dark Energy Stars in Finch-Skea Spacetime with a Schwarzschild-(Anti)-de Sitter Exterior. arXiv:2605.30398.
[9] Tullini, A. (2026). Boundedness and decay for the conformal wave equation in Schwarzschild-AdS under dissipative boundary conditions. arXiv:2604.02084.
[10] Friedrich, H. (1995). Einstein equations and conformal structure: existence of anti-de Sitter-type space-times. Journal of Geometry and Physics 17.2, pp. 125–184.
[11] Graf, O. & Holzegel, G. (2024). “Linear Stability of Schwarzschild-Anti-de Sitter spacetimes I: The system of gravitational perturbations”. arXiv:2408.02251.
[12] Moschidis, G. (2020). A proof of the instability of AdS for the Einstein-null dust system with an inner mirror, Analysis & PDE 13, no. 6, 1671–1754.
[13] Landau, L. D.; Lifshitz, E. M. (1971). The Classical Theory of Fields. Course of Theoretical Physics, Vol. 2. Translated from the Russian by M. Hamermesh (University of Minnesota). Pergamon Press: Oxford, New York, Toronto, Sydney, Braunschweig, p. 387.
[14] Shipov, G. (1998). The Theory of Physical Vacuum. Moscow ST-Center, Russia ISBN 5 7273-0011-8.
[15] Sedov, L. I. (1994). Continuum Mechanics, Vol. 1. Moscow: Nauka (in Russian).
[16] Batanov-Gaukhman, M. (2023). Geometrized Vacuum Physics. Part I. Algebra of Stignatures. Avances en Ciencias e Ingeniería, 14 (1), 1-26.

[17] Batanov-Gaukhman, M. (2023). Geometrized Vacuum Physics. Part II. Algebra of Signatures. Avances en Ciencias e Ingeniería, 14 (1), 27-55.
[18] Batanov-Gaukhman, M. (2023). Geometrized Vacuum Physics. Part III. Curved Vacuum Area. Avances en Ciencias e Ingeniería Vol. 14 nro 2 año 2023 Articulo 5.
[19] Batanov-Gaukhman, M. (2024). Geometrized Vacuum Physics Part VI: Hierarchical Cosmological Model, Avances en Ciencias e Ingeniería Vol. 14 nro 4 año 2023.
[20] Batanov-Gaukhman, M. (2025). Geometrized Vacuum Physics Part VII: "Electron" and "Positron", Avances en Ciencias e Ingeniería Vol. 15 nro 1 año 2024 Articulo 3.
[21] Zalaletdinov R. (2008). Averaging Problem in Cosmology and Macroscopic Gravity. International Journal of Modern Physics A. Vol. 23, No. 08, pp. 1173-1181 (2008) and arXiv:0801.3256.
[22] Buchert, T.; van Elst, H.; Heinesen, A. (2023). The averaging problem on the past null cone in inhomogeneous dust cosmologies. Gen. Rel. Grav. V. 55, 7 or arXiv:2202.10798v2.
[23] Green, S. R.; Wald, R. M. (2011). A new framework for analyzing the effects of small scale inhomogeneities in cosmology. Phys. Rev. D 83, 084020 or arXiv:1011.4920v2.
[24] Schleich, K. & Witt, D. M. (2009). A simple proof of Birkhoff's theorem for cosmological constant. *J. Math. Phys.* 51, 112502 (2010), arXiv:0908.4110.
[25] Schur, F. (1886). Ueber den Zusammenhang der Räume constanten Riemann'schen Krümmungsmaasses mit den projectiven Räumen. Mathematische Annalen, 27, pp. 537–567.
[26] Isaacson, R. A. (1968). Gravitational Radiation in the Limit of High Frequency. I. The Linear Approximation and Geometrical Optics. Physical Review, 166(5), 1263–1271. DOI: 10.1103/PhysRev.166.1263.
[27] Isaacson, R. A. (1968). Gravitational Radiation in the Limit of High Frequency. II. Nonlinear Terms and the Effective Stress Tensor. Physical Review, 166(5), 1272–1279. DOI: 10.1103/PhysRev.166.1272.
[28] Zel'dovich, Ya. B. (1968). The cosmological constant and the theory of elementary particles. Sov. Phys. Usp. 11, 381–393.
[29] Weinberg, S. (1989). The cosmological constant problem. Rev. Mod. Phys. 61, 1–23.